The Hyperfine Structure and Nuclear Magnetic Moment of Caesium I

L. P. GRANATH AND R. K. STRANATHAN, *Department of Physics, New York University, University Heights*

(Received July 16, 1935)

The hyperfine structure of the lines λλ8761, 4593, 4555, 3889 and 3877 of the arc spectrum of caesium were observed with a Fabry-Perot etalon. The interval factors for the $6^2S_{\frac{1}{2}}$, $6^2P_{\frac{1}{2}}$, $7^2P_{\frac{1}{2}}$, and $8^2P_{\frac{1}{2}}$ states were found to be 0.0767, 0.00925, 0.00329, and 0.0017 cm^{-1}, respectively. Assuming a nuclear spin of 7/2, the nuclear magnetic moments calculated from Goudsmit's formulas were 2.66, 2.38, 2.62, and 3.01 nuclear magnetons for the respective states.

INTRODUCTION

THE hyperfine structure of caesium was first investigated by Jackson,[1] but the accuracy of the work was not sufficiently great to warrant the calculation of magnetic moments from the more recently derived formulas.[2] Since that time several determinations have been made. The authors[3] obtained the hyperfine structure interval factor for the $6^2P_{\frac{1}{2}}$ state and from this calculated the nuclear magnetic moment, while Heydenburg[4] has obtained the separation factors of the $6^2P_{3/2}$ and $7^2P_{3/2}$ states from the polarization of resonance radiation. Jackson[5] has obtained the interval factors for the $6^2S_{\frac{1}{2}}$, $6^2P_{\frac{1}{2}}$, $6^2P_{3/2}$, $7^2P_{\frac{1}{2}}$ and $7^2P_{3/2}$ states.

The spin of caesium has been established as 7/2 by Kopfermann[6] from his work on the spark spectrum and by Cohen[7] from the atomic beam method.

This work is concerned with the determination of the interval factors of the $6^2S_{\frac{1}{2}}$, $6^2P_{\frac{1}{2}}$, $7^2P_{\frac{1}{2}}$ and $8^2P_{\frac{1}{2}}$ states, and the calculation of the corresponding nuclear magnetic moments.

APPARATUS AND METHOD

The arc spectrum of caesium was produced in a discharge tube of the type shown in Fig. 1. The caesium was obtained by heating a mixture of pulverized metallic calcium and caesium chloride in a glass tube sealed to the vacuum system. An inert gas, helium for the λ8761, both helium and argon for the λλ4593 and 4555 and argon for the λλ3877 and 3889 lines, was used to carry most of the discharge. Argon was necessary for the latter lines because the helium line at λ3888 was so close to the caesium doublets as to render microphotometering of the patterns impossible. The excitation was obtained by means of a 1500-volt d.c. generator. The voltage across the tube was lowered until the current was about 1/5 of that required to produce any observable reversal of the λ8521 ($6^2S_{\frac{1}{2}}-6^2P_{3/2}$) line which, under these conditions was about 0.2 ampere. The tube was cooled to a temperature of about 50°C by an air blast from a fan.

A special spectrograph was constructed with a lathe bed as a foundation. A 60° glass prism of index 1.75, a 76-cm focal length camera and a collimator from a Hilger constant deviation spectrograph were used in the construction. The advantage of this construction was its rigidity, all optical parts being mounted on the same foundation. The etalon was mounted between the collimator and the prism. Etalons of various sizes could be accommodated since the distance between prism and collimator was variable; and in addition all optical parts could be raised or lowered with respect to the lathe bed or to each other.

In order to eliminate changes in the optical system due to temperature fluctuations, the whole system, except the plateholder, was maintained at a constant temperature to within 0.1°C. It was important to adjust the etalon for parallelism at the same temperature at which it was to be used. This was accomplished by rotating the etalon stand until it came into line with light from a mercury arc which entered through a small window in the side of the constant temperature box.

[1] D. A. Jackson, Proc. Roy. Soc. **A121**, 432 (1928).
[2] S. Goudsmit, Phys. Rev. **43**, 636 (1933).
[3] L. P. Granath and R. K. Stranathan, Phys. Rev. **46**, 317 (1934).
[4] N. P. Heydenburg, Phys. Rev. **46**, 802 (1934).
[5] D. A. Jackson, Proc. Roy. Soc. **A147**, 500 (1934).
[6] H. Kopfermann, Zeits. f. Physik **73**, 437 (1932).
[7] V. W. Cohen, Phys. Rev. **46**, 713 (1934).

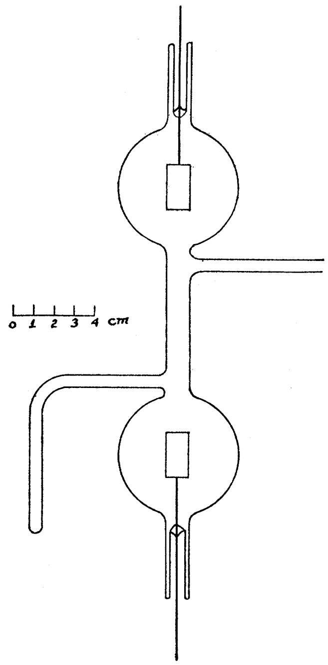

FIG. 1. Discharge tube.

For long exposures it was found necessary to eliminate changes in the index of refraction of air due to changes in atmospheric pressure. This was accomplished by placing the etalon in an aluminum chamber which could be made air tight. This chamber was used in photographing the λ8761 line which required an exposure time of about twelve hours. The separation of the components of this line is about 0.037 cm^{-1} and with a spacer of 2.5 cm, a change in pressure of 1 mm would cause the components to shift by 0.004 cm^{-1}. This is more than 1/10 the separation to be measured, consequently the pressure must be kept constant to better than this amount. This is impossible without the chamber, as the atmospheric pressure may vary by several millimeters during a twelve-hour exposure.

The etalon plates were of fused quartz and were silvered to provide a reflecting power of about 90 percent in the red. These silver surfaces were obtained by evaporating silver on the quartz surfaces in a vacuum. The reflecting power was measured by the method described by Childs.[8]

[8] W. H. J. Childs, J. Sci. Inst. 3, 97, 129 (1926).

MEASUREMENTS

λ8761 ($6^2P_{1/2}-6^2D_{3/2}$)

This line was photographed with hypersensitized I P plates. It photographed as a doublet, the separation due to the $6^2D_{3/2}$ state being too small to be observed. The results of the measurements are given in Table I, where the order numbers do not refer to the order of interference but are numbered outward from the center of the Fabry-Perot pattern.

It will be seen that the values for orders 3 and 4 of plates 143 and 144 are noticeable lower than those for the first two orders. This is believed to be due to the microphotometer since it did not appear in plate 140, which was adjusted for each order to allow for the curvature in the pattern (due to the prism curvature). This was also borne out by the I/e widths which were found larger for orders 3 and 4.

The microphotometer traces did not fall to the clear plate level between the components. In order to correct for the mutual influence of the position of one component on the other, the patterns were drawn out to linear scales of intensity and dispersion. To obtain a linear scale of intensity, an intensity calibration was made on each plate by the use of a wedge-shaped slit. Spectral photographs of the light from a tungsten lamp were microphotometered and a curve of galvanometer deflections *versus* slit widths plotted. Since the intensity was proportional to the slit

TABLE I. *Measured separations of components of λ8761 of Cs I. Spacer 2.504 cm.*

PLATE	ORDER	MEASURED $\Delta\nu$ cm^{-1}	CORRECTED $\Delta\nu$ cm^{-1}	DEVIATION FROM AVERAGE
140	1	0.0341	0.0352	0.0002
	2	0.0335	0.0346	0.0004
	3	0.0337	0.0348	0.0002
	4	0.0339	0.0350	0.0000
143	1	0.0340	0.0351	0.0001
	2	0.0342	0.0353	0.0003
	3	0.0322	0.0353	0.0003
	4	0.0310	0.0341	0.0009
144	1	0.0357	0.0368	0.0018
	2	0.0334	0.0345	0.0005
	3	0.0320	0.0351	0.0001
	4	0.0315	0.0346	0.0004
		Average	0.0350	0.0004

width, this curve was equivalent to galvanometer deflections *versus* intensity. From this graph the galvanometer deflections on the pattern were transformed into a linear scale of intensity.

The center of the pattern was obtained by measuring the mean distance between corresponding points of similar components on either side of the center. These measurements were made for various intensity heights and the average of the various mean values taken as the center of the pattern. It was impossible to obtain, on one trace, more than one or two orders on both sides of the center, hence it was necessary to take several traces of the pattern, duplicating the end components. The distances from the center of the pattern to both sides of all components were measured for various galvanometer deflections. These distances were measured from small galvanometer deflections, in steps of 1 or 2 mm, to the maximum galvanometer deflection. Upon squaring these distances from the center, the linear dispersion of the pattern was obtained.

The centers of the components were then determined and the $\Delta\nu$ found by dividing the distance between components by twice the product of the spacer thickness and the distance between orders.

To correct for the influence of one component on the position of the other, each line was assumed to have a Doppler form. If the intensity at the center of the first component is A_1 and that at the center of the second A_2; and if X_0 is the distance between centers and X is the distance from the center of the component of intensity A_1 to any point on either curve, it follows that

$$I = A_1 e^{-aX^2} + A_2 e^{-a(X-X_0)^2},$$

where $a^{-\frac{1}{2}}$ is the width at $I = A/e$. The difference between X_0 and the distance between maxima of the plotted curves is the amount to be added to give the true separation. As a check, the correction was determined by finding two empirical curves which, when added together, gave the experimental pattern. The corrected intervals are shown in Table I.

Comparator measurements were made upon a plate taken with a one-cm spacer and the un-

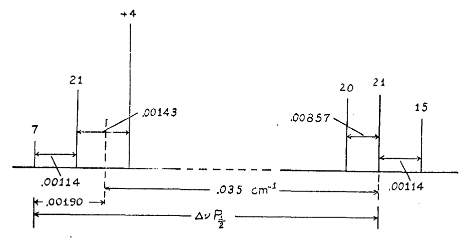

FIG. 2. Calculated pattern for the λ8761 line.

corrected interval found to be 0.034 cm^{-1}. Comparator measurements on plate 140 also checked the uncorrected values from the microphotometer traces.

The average value of the corrected separation between centers of gravity of the lines is 0.035 cm^{-1} and this is probably accurate to less than 0.001 cm^{-1}.

To obtain the separation of the $6^2P_{\frac{1}{2}}$ state from this value, the influence of the $6^2D_{3/2}$ state must be considered. The ratio of the interval factors for the $6^2D_{3/2}$ and $6^2P_{\frac{1}{2}}$ states was calculated from the relation[2]

$$a = \Delta\nu l(l+1)g(I)/Z_i(l+\tfrac{1}{2})j(j+1)1838$$

where $Z_i(D_{3/2}) = 45$ and $Z_i(P_{\frac{1}{2}}) = 50$. This gave $a(D_{3/2})/a(P_{\frac{1}{2}}) = 0.03085$. By using a nuclear spin of 7/2, diagrams of the pattern were constructed similar to the one shown in Fig. 2 for several assumed values of the interval factor of the $6^2P_{\frac{1}{2}}$ state. The amount to be added to the measured value to obtain the separation of the $6^2P_{\frac{1}{2}}$ state was noted in each case. The quantity to be added was found to be 0.002 cm^{-1}. The value of the $6^2P_{\frac{1}{2}}$ separation was then $0.035+0.002=0.037$ ± 0.001 cm^{-1}. This gives an interval factor of 0.00925 ± 3 percent. The proper values for Z_i are not well established; however, since Z_i appears only as a very small correction to the interval, a large error in it would produce an extremely small error in the interval factor.

λ4555 ($6^2S_{1/2} - 7^2P_{3/2}$) and λ4593 ($6^2S_{1/2} - 7^2P_{1/2}$)

These lines were investigated by using two spacers and silver surfaces on the etalon plates of about 90 percent reflecting power for these wavelengths. Eastman process plates were used and the exposure time ranged from 10 to 40 minutes for tube currents of 0.08 to 0.10 ampere. The lines appeared as doublets, the separation due to

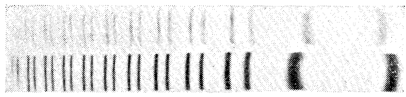

FIG. 3. Photograph of λ4593 and λ4555.

the $7^2P_{3/2}$ and $7^2P_{1/2}$ states being too small to be observed. A photograph of one of the patterns and a microphotometer trace are shown in Figs. 3 and 4. The $\Delta\nu$'s were calculated in a manner similar to that described for the λ8761 line, except that no intensity calibration was necessary and it was not necessary to plot the measured pattern.

The results of the measurements of the microphotometer traces are given in Tables II and III.

The observed separation is different for the two lines by 0.0079 cm^{-1}, this difference being due to the splitting of the 7^2P states. To obtain the interval factor for the $7^2P_{1/2}$ state from the observed data, diagrams were constructed as shown in Fig. 5 for various assumed values of the interval factor for the $7^2P_{1/2}$ and $7^2P_{3/2}$ states. These diagrams show that a small quantity must be added to the $6^2S_{1/2}$ separation to obtain the measured separation of the λ4593 line, and another small quantity must be subtracted from

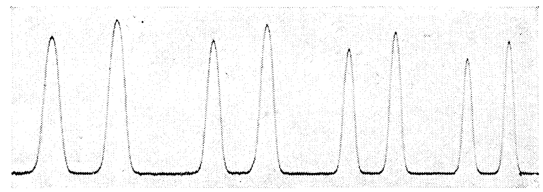

FIG. 4. Microphotometer trace of λ4555.

TABLE II. *Measured separations of components of λ4555 of Cs I.*

Plate	Spacer (cm)	$\Delta\nu$ (cm^{-1})	Deviation from final average
172	1.024	0.3029	0.0003
		.3029	.0003
		.3034	.0002
		.3030	.0002
		.3032	.0000
		.3033	.0001
		.3033	.0001
		.3032	.0000
		.3032	.0000
		Ave. 0.3032	
173	1.024	0.3036	0.0004
		.3034	.0002
		.3041	.0009
		.3033	.0001
		.3027	.0005
		.3034	.0002
		.3036	.0004
		.3036	.0004
		.3037	.0005
		.3035	.0003
		Ave. 0.3035	
235	0.9974	0.3034	0.0002
		.3031	.0001
		.3030	.0002
		.3030	.0002
		.3031	.0001
		.3033	.0001
		.3027	.0005
		.3029	.0003
		.3022	.0010
		.3022	.0010
		Ave. 0.3029	0.0003

Final average $\Delta\nu = 0.3032 \pm 0.0003$ cm^{-1}

TABLE III. *Measured separations of components of λ4593 of Cs I.*

Plate	Spacer (cm)	$\Delta\nu$ (cm^{-1})	Deviation from final average
235	0.9974	0.3111	0.0000
		.3116	.0005
		.3116	.0005
		.3116	.0005
		.3117	.0006
		.3118	.0007
		.3117	.0006
		.3115	.0004
		.3115	.0004
		.3113	.0002
		Ave. 0.3115	
170 *A*	1.024	0.3101	0.0010
		.3107	.0004
		.3110	.0001
		.3110	.0001
		.3121	.0010
		.3119	.0008
		.3109	.0002
		.3103	.0008
		.3107	.0004
		.3111	.0000
		Ave. 0.3110	
170 *B*	1.024	0.3111	0.0000
		.3111	.0000
		.3103	.0008
		.3112	.0001
		.3109	.0002
		.3108	.0003
		.3106	.0005
		.3107	.0004
		Ave. 0.3108	0.0004

Final average $\Delta\nu = 0.3111 \pm 0.0004$ cm^{-1}

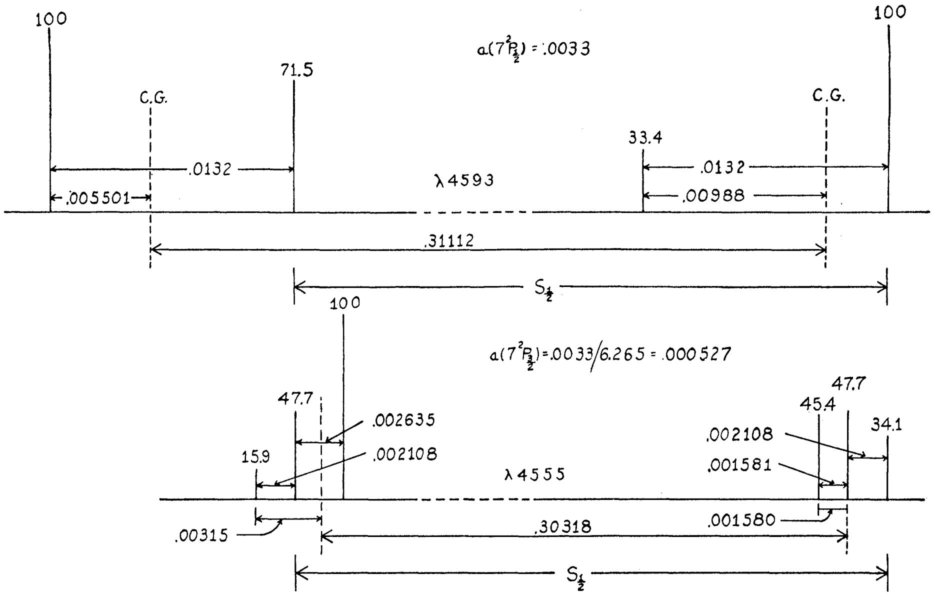

FIG. 5. Calculated pattern of λ4593 and λ4555.

the $6^2S_{\frac{1}{2}}$ separation to obtain the observed separation of the λ4555 line. The quantities to be added in one case and subtracted in the other were plotted against the respective interval factors as shown in Fig. 6. Next the ratio of the interval factors of the $7^2P_{\frac{1}{2}}$ and $7^2P_{3/2}$ states was calculated from the formula

$$g(I)=aZ_ij(j+1)(l+\tfrac{1}{2})\lambda 1838/\Delta\nu l(l+1)K$$

for $Z_i=55$, 51 and 45. For a given Z_i and a particular $a(P_{\frac{1}{2}})$ the difference in separation between the λ4593 and the λ4555 was calculated. This quantity is designated by $\Delta Sp_{\frac{1}{2}}-\Delta Sp_{3/2}$. It was plotted against various assumed values of the $7^2P_{\frac{1}{2}}$ interval factor with $Z_i=55$, 51 and 45.

This graph is shown in Fig. 7 and from it, that interval factor for the $7^2P_{\frac{1}{2}}$ state was selected which corresponded to the measured value of $\Delta Sp_{\frac{1}{2}}-\Delta Sp_{3/2}(0.0079\pm 0.0004\ \text{cm}^{-1})$. From the graph, the corresponding $7^2P_{\frac{1}{2}}$ interval factor using $Z_i=49.5$ is 0.00329 ± 0.00017 cm^{-1}. This Z_i was calculated from fine structure data. To see the dependence of $a(7^2P_{\frac{1}{2}})$ on Z_i, it was determined for $Z_i=55$ and a value of 0.00336 obtained.

In constructing the above diagrams, it was assumed that the calculated ratio of intensities is the same as was actually present in the radiation. This seems valid since all lines were photographed under conditions such that the λ8521 line exhibited no reversal. The "f values"[9] of the λ4500 and λ3800 lines are about 1/60 and 1/10,000 that of the f value for the λ8521 line and the reversal expected in these lines would be extremely small. The conclusion is also verified by the fact that the ratios of the intensities of the components of the λλ4555, 4593, 3877 and 3889 lines were as expected from theory.

The separation of the $6^2S_{\frac{1}{2}}$ state was obtained from the observed separation of the λλ4555 and 4593 lines. Taking $a(7^2P_{\frac{1}{2}})=0.00329\pm 0.00017$ cm^{-1} and referring to Fig. 6, it is found that $\Delta S_{\frac{1}{2}}$ is the measured separation of λ4593 minus 0.00436 ± 0.00020 or 0.3067 ± 0.0004 cm^{-1}. This gives an interval factor of 0.0767 ± 0.0001 cm^{-1} for the $6^2S_{\frac{1}{2}}$ state.

λ3889($6^2S_{1/2}-8^2P_{1/2}$) and λ3877($6^2S_{1/2}-8^2P_{3/2}$)

These lines were also observed as doublets. The exposure times were from 1 to 8 hours using Eastman 33 plates, a tube current of from 0.3 to 0.5 ampere, and reflecting powers of

[9] S. A. Korff and G. Breit, Rev. Mod. Phys. 4, 471 (1932).

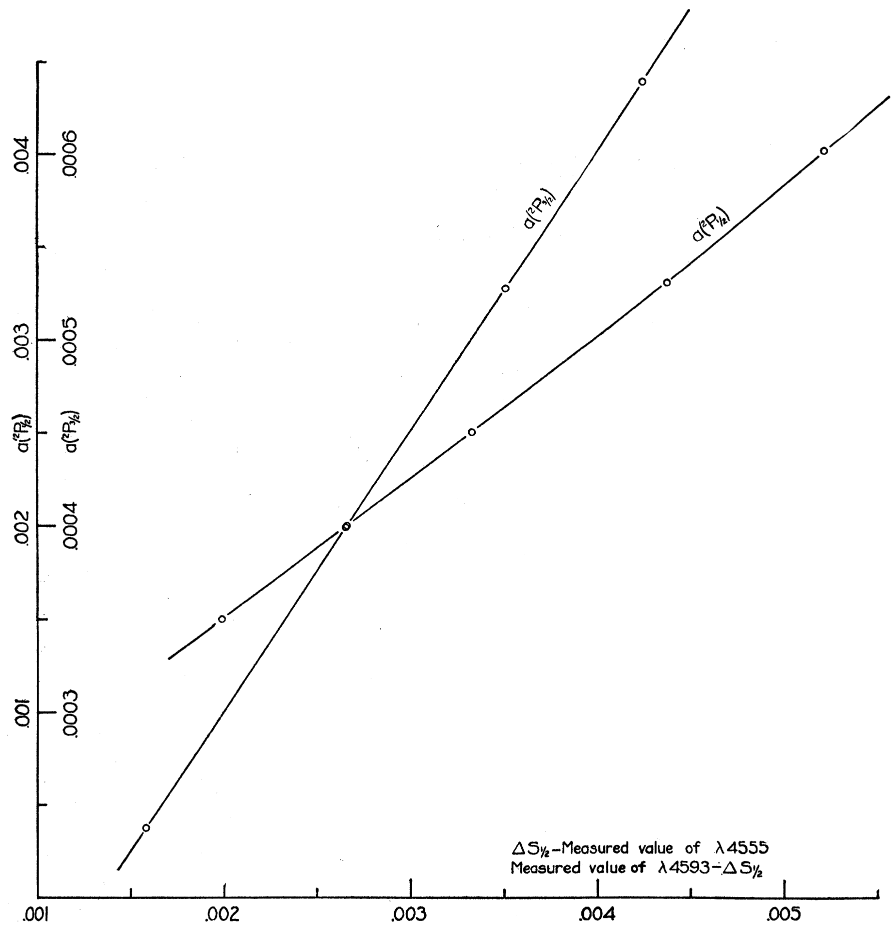

FIG. 6. Difference between centers of gravity and $\Delta 6^2S_{\frac{1}{2}}$ plotted against $a(P_{\frac{1}{2}})$ and $a(P_{3/2})$.

about 80 percent for these wave-lengths. The results of the measurements are given in Table IV.

These measurements are not considered as accurate as those for the 4500 lines. Due to the weak intensity it was necessary to use coarse grained plates which did not microphotometer as well as the process plates. The lines were wider due to the larger tube current and also due to lower resolving power in this region. On only a few plates was the intensity sufficient to obtain usable microphotometer traces, consequently most of the measurements were obtained by use of a comparator.

The interval factor for the $8^2P_{\frac{1}{2}}$ state was obtained from the measurements in the same manner as was described for the $7^2P_{\frac{1}{2}}$ state and was found to be 0.0017 ± 0.0003 cm^{-1}.

TABLE IV. *Measured separation of components of λλ3877 and 3889 of Cs I.*

Instrument	Plate	Spacer	Number of orders measured	$\Delta\nu$ (cm^{-1})
		λ3877		
Microphotometer	228	0.9974	9	0.3058
Comparator	200	.9974	12	.3062
"	231	.9974	18	.3052
"	241	.9974	16	.3051
				Ave. 0.3056 ± 0.0006
		λ3889		
Microphotometer	226	0.9974	9	0.3099
Comparator	230	.9974	18	.3091
"	209	1.024	14	.3104
"	229	.9974	8	.3094
				Ave. 0.3097 ± 0.0007

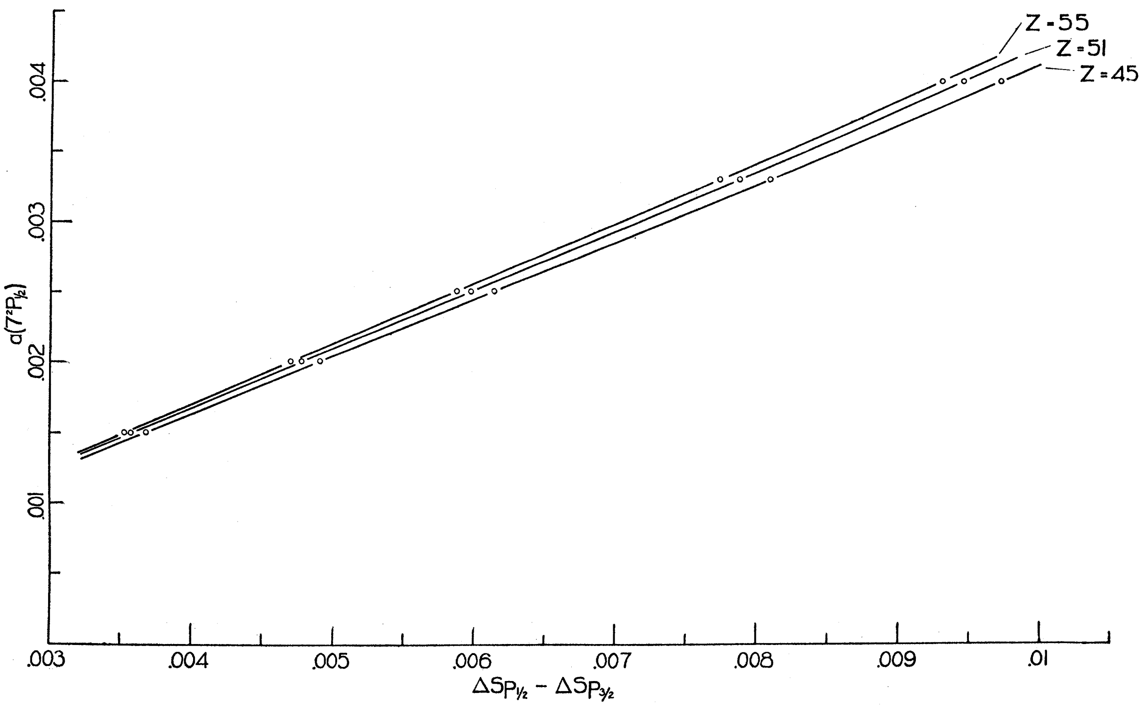

FIG. 7. $a(P_{\frac{1}{2}})$ plotted as a function of $\Delta SP_{\frac{1}{2}} - \Delta SP_{3/2}$.

CONCLUSION

The "g values" and hence the nuclear magnetic moments were calculated from Goudsmit's formulas, using the measured interval factors, the Z_i values for the P states as calculated from fine structure data and the corresponding relativity corrections. The results of these calculations are shown in Table V.

The percentage error has been given for the interval factors only, since the formulas available, at present, for the calculation of the magnetic moments may be in error by a magnitude comparable to the experimental error.

TABLE V. *Calculated g values and nuclear magnetic moments of Cs I.*

STATE	INTERVAL FACTOR (cm^{-1})	% ERROR	Z_i	$g(I)$	NUCLEAR MAGNETIC MOMENT
$6^2S_{\frac{1}{2}}$	0.0767	0.2	55	0.76	2.66
$6^2P_{\frac{1}{2}}$	0.00925	3	49.5	0.68	2.38
$7^2P_{\frac{1}{2}}$	0.00329	5	49.5	0.75	2.62
$8^2P_{\frac{1}{2}}$	0.0017	20	48.5	0.86	3.01

It is of interest to compare these results with those obtained by Heydenburg[4] from polarization of resonance radiation. He obtains a value of 0.00142 ± 5 percent for $a(6^2P_{3/2})$ and 0.000486 ±3 percent for $a(7^2P_{3/2})$. By using his values for the $^2P_{3/2}$ states and the authors' values for the $^2P_{\frac{1}{2}}$ states the ratio $a(6^2P_{\frac{1}{2}})/a(6^2P_{3/2})=6.52$ ±5 percent and the ratio $a(7^2P_{\frac{1}{2}})/a(7^2P_{3/2})$ $=6.80\pm5$ percent. The theoretical value of this ratio is 6.5 for $Z_i=55$ or 6.265 for $Z_i=51$.

It appears that the most probable value of $g(I)$ is between 0.68 and 0.75 and that it is the same for all the states considered within the limit of experimental error.

In conclusion the authors wish to express their appreciation to Professors G. Breit, and A. C. G. Mitchell for many helpful suggestions; and to the National Research Council for aiding this work with a research grant.

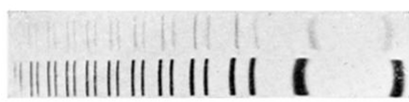

FIG. 3. Photograph of λ4593 and λ4555.

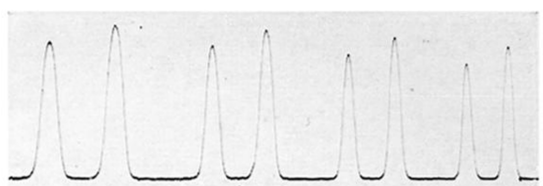

FIG. 4. Microphotometer trace of λ4555.